ISSN (Print) 1226-1750
ISSN (Online) 2233-6656
Journal of Magnetics 28(4), 352-360 (2023) https://doi.org/10.4283/JMAG.2023.28.4.352

Study on Calculation Method of D-Axis Super-Transient Reactance of Damped Winding Permanent Magnet Electrical Machine

Yujing Guo*, Bin Shi, and Ping Jin

College of Energy and Electrical Engineering, Hohai University, Nanjing 211100, China

(Received 13 February 2023, Received in final form 23 September 2023, Accepted 29 September 2023)

Dynamic parameters directly reflect the dynamic performance of electrical machines. In this paper, two methods for calculating the d-axis super-transient reactance of a damped winding permanent magnet electrical machine (DWPMEM) are proposed. One is the analytical method: the analytical model of d-axis super-transient reactance is developed, and the d-axis super-transient reactance is calculated by taking the coupling of permanent magnet (PM) and winding current magnetic field into account. The other is the parameter identification method: the parameter identification model of DWPMEM is established, and the reactance is identified based on the DC step voltage method. The calculation accuracy of the two methods is verified by the measured data, and the variation rules of the d-axis super-transient reactance with damping winding structures are analyzed. The work of this paper has a certain reference value for the design and dynamic operation evaluation of DWPMEM.

Keywords : damping winding, PM electrical machine, super-transient reactance, analytical method, parameter identification

1. Introduction

Dynamic parameters including reactance and time constants can directly reflect the dynamic performance of electrical machines under special working conditions [1], therefore they have been important research contents in the electrical machine and the related fields. The super-transient reactance is one important dynamic parameter of the electrical machine, which can determine the maximum value of sudden short-circuit current. Therefore, its accurate calculation has a great influence on the electrical machine state evaluation.

When the structure parameters can be provided, analytical and finite element methods are good choices to calculate the electrical machine dynamic parameters. An analytical method is used to calculate the dynamic parameters of the salient pole generator in [2-4]. The super-transient reactance parameters of salient pole generators with different damping winding materials and structures are calculated and studied by the finite element method in [5] and [6]. And the super-transient reactance is studied based on d-axis flux and current by using the superconducting loop method in [7].

When the structure parameters are unknown, the d-axis transient reactance can only be obtained by the parameter identification method. Three-phase sudden short-circuit method is a commonly used method for transient parameter identification [8], but the current impulse caused by this method brings damage risk to the electrical machine [9]. In [10] and [11], the electrical machine transient parameters are identified based on the DC step voltage method and the sinusoidal voltage method respectively. Accurate dynamic parameters can be obtained without damaging the electrical machine by using the two methods.

Compared with the traditional synchronous electrical machine, permanent magnet (PM) electrical machine (PMEM) has a simpler structure, higher efficiency, and higher power density, therefore it is widely used in the industry field [12]. Damped winding PM electrical machine (DWPMEM) can produce stable torque or output stable electric energy at low speed, and the magnetic field generated by damping winding current can effectively weaken the magnetic field negative sequence and improve the dynamic stability of the electrical machine in the dynamic process [13]. Therefore, it has a good application

*Corresponding author: Tel: +8613485119828
Fax: +8613485119828, e-mail: yjguo@hhu.edu.cn

prospect in the fields of marine propulsion, wind power generation, etc. However, due to the magnetic field variation, the DWPMEM dynamic parameter calculation method and its influencing factors are different from that of electric excitation damping winding electrical machines [14], but there are few reports about the relevant research content at present.

In this paper, DWPMEM is taken as the research object, and the calculation method and influencing factors of its super-transient reactance are studied. The analytical calculation model of DWPMEM d-axis super-transient reactance is proposed based on the superconducting loop method in section II. The parameter identification model is established and used to identify the parameters of d-axis super-transient reactance in section III. The accuracy of the two calculation methods is verified by experiments in section IV. The variation rules of d-axis super-transient reactance with damping winding structures are investigated in section V. And at last, some important conclusions are provided in section VI.

The main innovations of this paper are as follows: 1) The DWPMEM d-axis super-transient reactance analytical calculation model is proposed, and the coupling of the magnetic field produced by PM and stator winding current is considered in the model. 2) The identification model of DWPMEM super-transient reactance is established, based on which the super-transient reactance can be obtained accurately without electrical machine structure parameters.

2. Analytical Calculation Model of D-Axis Super-Transient Reactance

2.1. Calculation model of super-transient reactance

The flux equations of DWPMEM are different from those of electric excitation electrical machine due to PM excitation, and its equations are as follows [15],

$$\begin{cases} \psi_d = -X_d i_d + B \cdot S_m + X_{ad} i_{1d} \\ \psi_{fd} = B \cdot S_m \\ \psi_{1d} = -X_{ad} i_d + B \cdot S_m + X_{11d} i_{1d} \end{cases}. \tag{1}$$

The voltage equation is

$$0 = p\psi_{1d} + R_{1d} i_{1d}, \tag{2}$$

where ψ_d, ψ_{fd} and ψ_{1d} are the d-axis flux generated by stator winding, PM, and damping winding respectively. X_d, X_{ad}, X_{11d} and R_{1d} are the d-axis components of stator winding reactance, stator armature reaction reactance, damping winding reactance and damping winding resistance respectively. i_d and i_{1d} are the d-axis current components of stator winding and damping winding respectively. B and S_m are the PM d-axis magnetic flux density and the cross-sectional area of the magnetic circuit respectively.

According to Eqs. (1) and (2), it can be obtained

$$\begin{cases} \psi_d = -X_d i_d + B \cdot S_m + X_{ad} i_{1d} \\ \psi_{fd} = B \cdot S_m \\ 0 = -X_{ad} i_d + B \cdot S_m + (X_{11d} + R_{1d}/p) i_{1d} \end{cases}. \tag{3}$$

The corresponding d-axis equivalent magnetic circuit is shown in Fig. 1. In the figure, X_L and X_{1dL} are the leakage reactance of stator winding and d-axis damping winding respectively, and

$$X_L = X_d - X_{ad}, \tag{4}$$

$$X_{1dL} = X_{11d} - X_{ad}. \tag{5}$$

According to the principle of the superconducting loop method [1, 11], it can be assumed that, the flux is unchanging before and after short-circuit fault, the resistance element can be ignored, the voltage source can be short-circuited, and the current source can be open-circuited. Therefore, the equivalent circuit for d-axis super-transient reactance calculation is obtained as shown in Fig. 2.

The parameter X_d'' can be expressed as

$$X_d'' = X_L + \frac{1}{\frac{1}{X_{ad}} + \frac{1}{X_{1dL}}}. \tag{6}$$

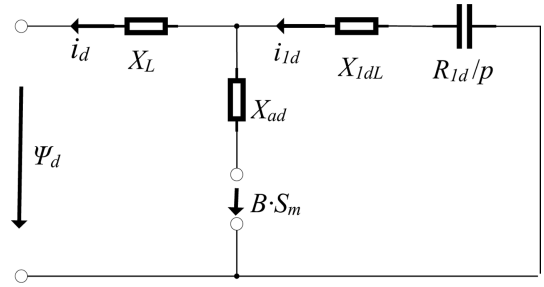

Fig. 1. D-axis equivalent magnetic circuit.

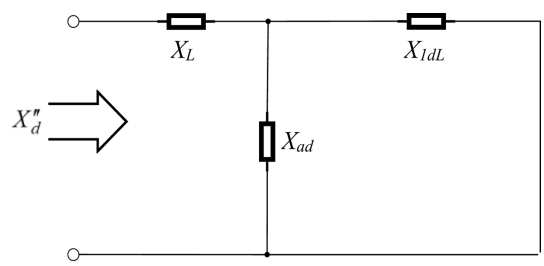

Fig. 2. The equivalent circuit for d-axis super-transient reactance calculation.

Substituting eqs. (4) and (5) into (6), the expression of d-axis super-transient reactance can be obtained:

$$X_d'' = X_L + X_{ad} - \frac{X_{ad}^2}{X_{11d}}. \tag{7}$$

It can be obtained from the above equation that the d-axis super-transient reactance is related to the stator winding leakage reactance, the d-axis stator armature reaction reactance, and the d-axis damping winding reactance.

2.2. Calculation of relevant reactance parameters

When the fundamental magnetic flux generated by the winding current is considered only, the self-induction of the a-phase winding is

$$L_{aa} = L_0 + L_2 \cos 2\gamma, \tag{8}$$

$$L_0 = L_{0L} + \frac{2w^2\tau L\lambda_0}{P\pi^2 a_s^2} k_{w1}^2, \tag{9}$$

$$L_2 = \frac{2w^2\tau L\lambda_2}{P\pi^2 a_s^2} k_{w1}^2, \tag{10}$$

where L_0 and L_2 are the self-induction fundamental component and quadratic component respectively. γ is the included electrical angle between the rotor d-axis and the a-axis phase. w, τ, L, P, a_s and k_{w1} are the total number of phase winding turns, pole pitch, stator core length, number of pole pairs, number of winding parallel branches, and winding coefficient respectively.

When the d-axis of the rotor coincides with the a-phase winding axis, namely $\gamma = 0$, then

$$L_{aa} = L_0 + L_2 = L_{0L} + L_{aads}, \tag{11}$$

$$L_{aads} = \frac{4w^2\tau L}{P\pi^2 a_s^2} k_{w1}^2 \lambda_{d11}, \tag{12}$$

where L_{0L}, L_{aads} and λ_{d11} are the leakage flux inductance coefficient, main flux a-phase winding inductance coefficient, and the d-axis equivalent magnetic permeability coefficient respectively.

The magnetic motive force generated by PM is

$$F_c = H_c h_{Mp}, \tag{13}$$

where H_c is the PM coercivity, and h_{Mp} is the magnetization direction length.

When the magnetic flux generated by PM is considered only, the a-phase fundamental component flux linkage is

$$\psi_{afd} = \frac{2w\tau L}{\pi a_s} H_c h_{Mp} \lambda_{d1} k_{w1} \cos\gamma, \tag{14}$$

where λ_{d1} is the air-gap permeability coefficient.

The a-phase winding mutual inductance is

$$M_{afd} = \frac{2w\tau L}{\pi a_s} \lambda_{d1} k_{w1} \cos\gamma. \tag{15}$$

When $\gamma = 0$

$$M_{afds} = \frac{2w\tau L}{\pi a_s} \lambda_{d1} k_{w1}. \tag{16}$$

Regardless of the saturation effect, the a-phase inductance with the coupled magnetic field generated by the winding current and the PM is

$$L_{aad} = L_{aads} + M_{afds}, \tag{17}$$

$$L_{aad} = \frac{4w^2\tau L}{P\pi^2 a_s^2} k_{w1}^2 \lambda_{d11} + \frac{2w\tau L}{\pi a_s} k_{w1} \lambda_{d1}. \tag{18}$$

Therefore, the d-axis stator armature reaction inductance is

$$L_{ad} = \frac{3w\tau L}{\pi a_s} k_{w1} \left(\frac{2w}{P\pi a_s} k_{w1} \lambda_{d11} + \lambda_{d1}\right). \tag{19}$$

The d-axis stator armature reaction reactance is

$$X_{ad} = 2\pi f \frac{3w\tau L}{\pi a_s} k_{w1} \left(\frac{2w}{P\pi a_s} k_{w1} \lambda_{d11} + \lambda_{d1}\right), \tag{20}$$

where f is electric frequency.

Similarly, when the magnetic field generated by the stator winding current is considered only, the self-inductance coefficient of the damping winding is

$$L_{11ds} = \frac{2w_{1d}^2\tau L}{P\pi^2 a_{1d}^2} \sum_j \left\{ \sum_{2L=|k-j|} \frac{\lambda_{2L}}{kj} \sin\frac{k\beta_{1d}\pi}{2} \sin\frac{j\beta_{1d}\pi}{2} + \sum_{2L=|k+j|} \frac{\lambda_{2L}}{kj} \sin\frac{k\beta_{1d}\pi}{2} \sin\frac{j\beta_{1d}\pi}{2} \right\}, \tag{21}$$

where λ_{2L} is the d-axis equivalent magnetic permeability coefficient.

When the magnetic field generated by PM is considered only, the mutual inductance coefficient of the damping winding is

$$M_{1fds} = \frac{2w_{1d}\tau L}{\pi a_{1d}} \sum_k \frac{\lambda_{dk}}{k} \sin\frac{k\beta_{1d}\pi}{2}, \tag{22}$$

where w_{1d}, β_{1d} and a_{1d} are the number of damping windings, damping winding short-pitch ratios, and damping winding parallel branches respectively; λ_{dk} is the permeability coefficient for the magnetic field generated by winding current.

Regardless of the saturation effect, the d-axis damping winding inductance with the coupled magnetic field can be obtained by eq. (23).

$$L_{11d}=\frac{2w_{1d}\tau L}{\pi a_{1d}}\left\{\frac{w_{1d}}{P\pi a_{1d}}\sum_{j}\left[\sum_{2L=|k-j|}\frac{\lambda_{2L}}{kj}\sin\frac{k\beta_{1d}\pi}{2}\sin\frac{j\beta_{1d}\pi}{2}+\sum_{2L=|k+j|}\frac{\lambda_{2L}}{kj}\sin\frac{k\beta_{1d}\pi}{2}\sin\frac{j\beta_{1d}\pi}{2}\right]+\sum_{k}\frac{\lambda_{dk}}{k}\sin\frac{k\beta_{1d}\pi}{2}\right\}. \quad (23)$$

Thus, the d-axis damping winding reactance is

$$X_{11d}=2\pi fL_{11d}. \quad (24)$$

The stator winding leakage reactance is composed of stator slot leakage reactance, stator harmonic leakage reactance, and stator end-winding leakage reactance.

$$X_L=X_{Ls}+X_{Lh}+X_{Le}. \quad (25)$$

In this paper, C_e is defined as the leakage reactance coefficient

$$C_e=\frac{4\pi f\mu 0(wk_{w1})^2LP_N}{mpU_N^2}, \quad (26)$$

where P_N and U_N are the rated power and rated voltage of the electrical machine respectively.

The stator slot leakage reactance is

$$X_{Ls}=\frac{2mp\lambda_s}{Z\beta_{1d}^2}C_e, \quad (27)$$

where λ_s is stator slot leakage permeance per unit, m is the number of phases and Z is the number of stator slots.

The stator harmonic leakage reactance is

$$X_{Lh}=\frac{m\tau\lambda_h}{\pi^2\beta_{1d}^2\delta_s}C_e, \quad (28)$$

where λ_h is stator harmonic leakage permeance per unit, and δ_s is the effective length of air gap.

The stator end-winding leakage reactance is

$$X_{Le}=0.67\frac{(L-0.64\tau)}{L\beta_{1d}^2}C_e. \quad (29)$$

3. Identification Calculation of D-Axis Super-Transient Reactance

The parameter identification method obtains the required identification results by applying specific excitation signals and combining the response waveform with the identification model [16-19]. The identification model of d-axis super-transient reactance is developed based on flux linkage and voltage equations in this section. According to the procedure shown in Fig. 3, the d-axis super-transient reactance is calculated: firstly, the d-axis current is calculated by finite element method and the d-axis current curve is fitted by genetic algorithm, and then the correlation coefficient is obtained and substituted into the d-axis super-transient reactance identification model. Finally, the d-axis super-transient reactance is calculated.

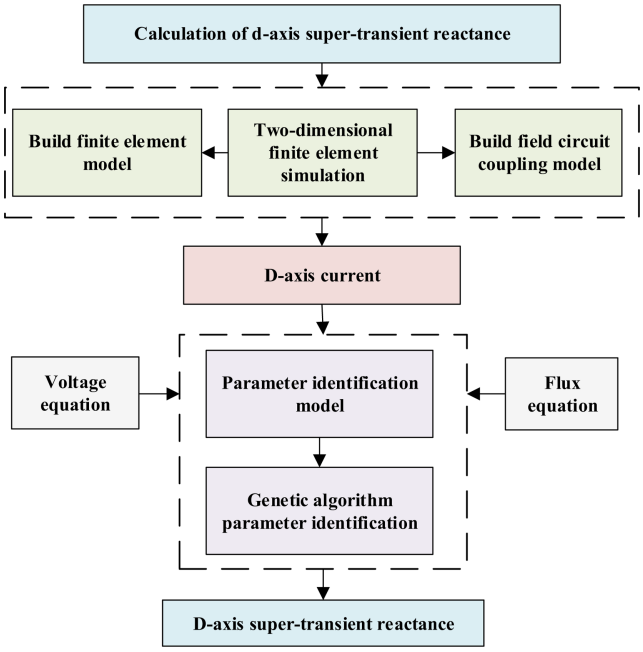

Fig. 3. (Color online) Calculation flow of d-axis super-transient reactance based on parameter identification.

3.1. Parameter identification model

By using the Laplace transform, the flux and voltage equations of PMEM in the frequency domain are obtained as follows:

$$\begin{cases}\Psi_d=-X_dI_d+B\cdot S_m+X_{ad}I_{1d}\\ \Psi_{fd}=B\cdot S_m\\ \Psi_{1d}=-X_{ad}I_d+B\cdot S_m+X_{11d}I_{1d}\end{cases}, \quad (30)$$

$$0=s\Psi_{1d}-\Psi_{1D0}+R_{1d}I_{1d}, \quad (31)$$

where s is the Laplace differential operator.

Substituting eq. (31) into eq. (30), it can be got that

$$\begin{cases}\Psi_d=-X_dI_d+B\cdot S_m+X_{ad}I_{1d}\\ \Psi_{fd}=B\cdot S_m\\ \Psi_{1D0}/s=-X_{ad}I_d+B\cdot S_m+(X_{11d}+R_{1d}/s)I_{1d}\end{cases}. \quad (32)$$

The d-axis stator winding flux can be expressed as

$$\Psi_d=-X_d(s)I_d+G_D(s)\Psi_{1D0}+G_f(s)B\cdot S_m, \quad (33)$$

where $X_d(s)$ is the d-axis operational reactance equipped

with damping windings; $G_D(s)$ and $G_f(s)$ are the transfer functions corresponding to the d-axis damping winding and the PM respectively.

The d-axis operational reactance equipped with damping windings $X_d(s)$ is

$$X_d(s) = X_d \cdot \frac{s(X_{11d} - \frac{X_{ad}^2}{X_d}) + R_{1d}}{sX_{11d} + R_{1d}}. \tag{34}$$

Substituting $X_{11d} - \frac{X_{ad}^2}{X_d} = X'_{11d}$ into eq. (34), then

$$X_d(s) = X_d \cdot \frac{sX'_{11d} + R_{1d}}{sX_{11d} + R_{1d}} = X_d \cdot \frac{sT'_D + 1}{sT_D + 1}, \tag{35)]}$$

where T_D and T'_D are the d-axis steady-state and transient time constants respectively.

The d-axis damping winding transfer function $sG_D(s)$ is

$$sG_D(s) = \frac{X_{ad}}{X_{11d} + \frac{R_{1d}}{s}} = \frac{X_{ad}}{R_{1d}} \cdot \frac{s}{sT_D + 1}. \tag{36}$$

The PM transfer function $G_f(s)$ is

$$G_f(s) = 1 - \frac{X_{ad}}{R_{1d}} \cdot \frac{s}{sT_D + 1}. \tag{37}$$

When the electrical machine is equipped with damping winding, the initial value of the d-axis operational reactance is the d-axis super-transient reactance, therefore,

$$X''_d = \lim_{s\to\infty} X_d(s) = X_d \cdot \frac{T'_D}{T_D}. \tag{38}$$

Add the DC step signal to the identification model of the d-axis super-transient reactance parameters. The frequency domain expression of the DC step voltage is

$$V_d(s) = \frac{V_d}{s}. \tag{39}$$

Therefore, the d-axis voltage equation is

$$V_d(s) = sX_d(s)I_d(s) + r_s I_d(s). \tag{40}$$

And then, it can be got

$$\frac{V_d}{s} = s \cdot X_d \cdot \frac{sT'_D + 1}{sT_D + 1} I_d(s) + r_s I_d(s). \tag{41}$$

The frequency domain expression of the d-axis current is

$$I_d(s) = \frac{V_d}{X''_d} \cdot \frac{s + \frac{1}{T_D}}{s^3 + (\frac{1}{T'_D} + \frac{1}{T_D})s^2 + \frac{r_s}{X''_d T_D} s}. \tag{42}$$

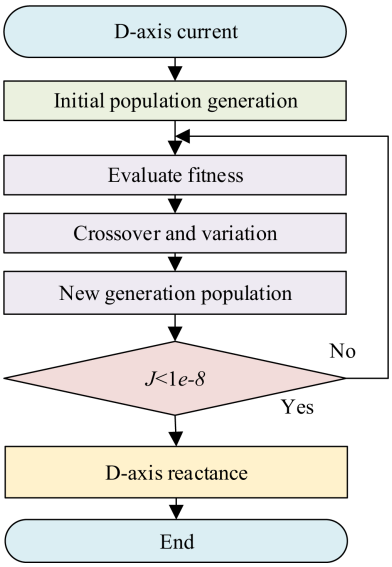

Fig. 4. (Color online) Parameter identification flow chart of genetic algorithm.

3.2. Parameter identification based on genetic algorithm

The time domain general solution of eq. (42) is

$$I_d(t) = C_1 e^{-\lambda_1 t} + C_2 e^{-\lambda_2 t} + C_3. \tag{43}$$

Based on eqs. (42) and (43), the d-axis super-transient reactance can be expressed as follows

$$X''_d = \frac{V_d}{C_1\lambda_2 + C_2\lambda_1 + C_3(\lambda_1 + \lambda_2)}, \tag{44}$$

where $C_3 = I_d(\infty)$.

It can be seen, that the corresponding coefficients in eqs. (43) and (44) are the same, therefore, the d-axis super-transient reactance can be obtained after the d-axis current is identified.

In this paper, a genetic algorithm is used for parameter identification, and the flow chart is shown in Fig. 4.

The fitness function is set as

$$J = \sqrt{\frac{\sum_{i=1}^{N} [I_d(t_i) - C_1 e^{-\lambda_1 t_i} - C_2 e^{-\lambda_2 t_i} - I_{d(\infty)}]^2}{N}}, \tag{45}$$

where C_1, λ_1, C_2 and λ_2 are the fitting coefficients, the subscript i represents the ith measurement point, and N is the total number of measurement points.

In this paper, the genetic algorithm population size and the fitness function value are set to 200 and $1e^{-8}$ respectively. When there is no improvement after 1000 iterations, the iteration is terminated, and the fitting coefficients are obtained.

4. Experimental Verification

4.1. Prototype structure

In order to verify the accuracy of the calculation model, a 1.1 kW DWPMEM is selected as the experiment prototype. As shown in Fig. 5(a), it adopts a flux-concentrated structure and each magnetic pole is composed of two PMs between which a magnetic bridge is arranged. The damping winding is evenly distributed in the outer layer of the rotor and the stator windings are arranged in a single layer. The pictures of the stator and rotor are shown in Fig. 5(b) and 5(c) respectively.

The main parameters of DWPMEM are shown in Table 1.

4.2. Calculation Results of analytical and parameter identification methods

The analytical method calculation results of d-axis super-transient reactance are shown in Table 2.

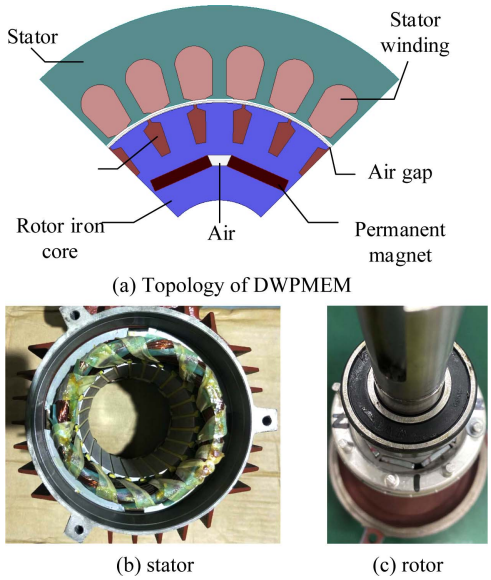

Fig. 5. (Color online) Topology of DWPMEM

Table 1. Main parameters of DWPMEM.

Parameter	Value
Rated power/kW	1.1
Voltage/V	380
Speed/r/min	1500
Current/A	2
Pole pairs	2
Number of slots	24
Stator inner diameter/mm	80
Rotor outer diameter/mm	130
Number of damping windings	20

Table 2. Analytical method calculation results.

Parameter	Value
D-axis stator armature reaction inductance/mH	3.3863
D-axis damping winding inductance/mH	0.0331
Stator winding leakage inductance/mH	0.0034
D-axis super-transient reactance/p.u.	0.1386

The finite element model of DWPMEM is set up and the d-axis current is calculated. The magnetic field distribution in the electrical machine is shown in Fig. 6. The d-axis current data are fit by the parameter identification method and the super-transient reactance can be obtained based on the fitting coefficients.

As shown in Fig. 7, the current waveforms obtained by finite element and parameter identification method can

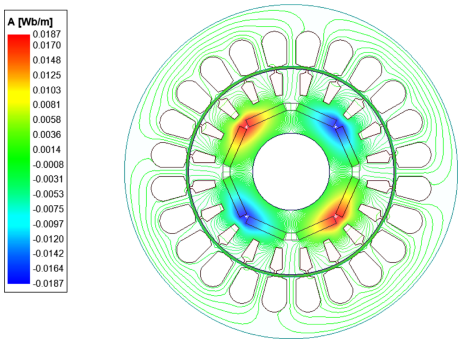

Fig. 6. (Color online) Magnetic field distribution in DWPMEM.

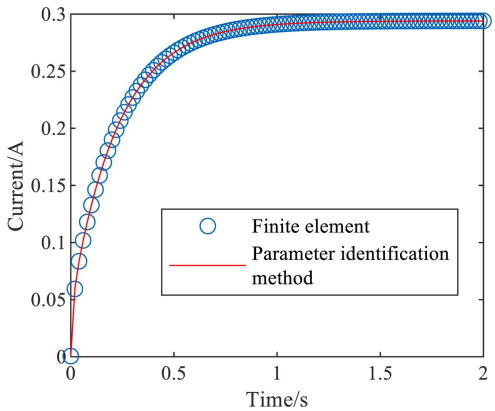

Fig. 7. (Color online) Identification and finite element results.

Table 3. Parameter identification results.

Fitting coefficient	Identification result	Fitting coefficient	Identification result
C_1	-0.0944	λ_1	20.1701
C_2	-0.1986	λ_2	4.4328
C_3	0.294	X''_d	0.14222p.u.

agree well with each other. The fitting coefficients and d-axis super-transient reactance are shown in Table 3.

4.3. DC step voltage method verification

The d-axis super-transient reactance experimental measurement method proposed in [18, 19] has high accuracy, and the measurement error is about 5 %. Therefore, in this paper, it is used for the d-axis super-transient parameter measurement. The experimental platform is shown in Fig. 8, which is mainly composed of DWPMEM, DC step voltage source, switch, etc.

During the experiment, the rotor d-axis is aligned with the axis of one-phase winding, the DC step voltage signal is applied to two-phase stator windings, the three-phase currents are measured, and the d-axis current is finally obtained by Park transformation. The d-axis current data obtained by the parameter identification method and the measured one is shown in Fig. 9. It can be seen, that although there are some white noises in the measured one, the data obtained by the two methods are basically consistent.

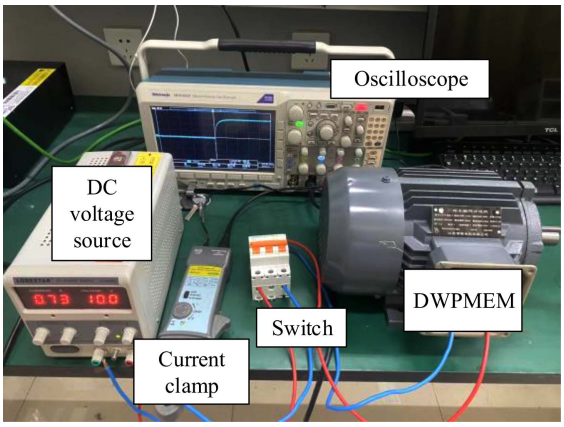

Fig. 8. (Color online) Experimental platform.

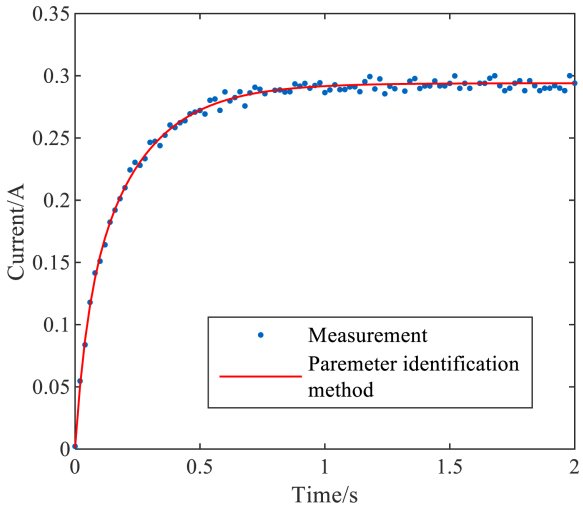

Fig. 9. (Color online) Identification and measurement data.

Table 4. Parameter identification results.

Fitting coefficient	Identification result	Fitting coefficient	Identification result
C_1	-0.0923	λ_1	21.8703
C_2	-0.2007	λ_2	4.4564
C_3	0.294	X''_d	0.13523p.u.

Table 5. Comparison of D-axis super-transient reactance.

X''_d	Value	Error
Analytical method	0.13860p.u.	2.44 %
Parameter identification method	0.14222p.u.	4.91 %
Measurement	0.13523p.u.	-

Table 4 lists the measurement data identification results of fitting coefficients and d-axis super-transient reactance.

Table 5 shows the d-axis super-transient reactance values obtained by analytical method, parameter identification method, and measurement respectively.

Taking the measurement result as the basic value, it can be seen from the table, that the analytical method calculation result is almost the same as the measured one (the error between them is 2.44 %), and the error between the parameter identification result and the experimental one is 4.91 %, which indicate the two methods have relatively high calculation accuracy. It should be pointed out that, if the experimental data are denoised, the error will be further reduced.

5. Study of Influence Factors

The d-axis super-transient reactance with different numbers of damping windings and short-pitch ratios are

Table 6. D-axis super-transient reactance with different number of damping windings.

Number of damping windings	Parameter identification method	Analytical method
16	0.15605p.u.	0.1512p.u.
17	0.15434p.u.	0.1463p.u.
18	0.14763p.u.	0.1429p.u.
19	0.14312p.u.	0.1401p.u.
20	0.14222p.u.	0.1386p.u.
21	0.13549p.u.	0.1321p.u.
22	0.13175p.u.	0.1266p.u.
23	0.12803p.u.	0.1232p.u.
24	0.11146p.u.	0.1101p.u.

calculated and analyzed in this section.

The d-axis super-transient reactance with different numbers of damping windings is calculated by using the analytical method and parameter identification method, and the calculation results are shown in Table 6 and Fig. 10.

From Table 6, it can be seen that the d-axis super-transient reactance decreases with the increasing damping winding number. This is because the increase in the number of damping windings narrows the magnetic circuit, reduces magnetic conductivity, and correspondingly reduces the relevant reactance parameters [20, 21]. The conclusion is the same as the one obtained based on eqs. (7) and (23).

As can be seen in Fig. 10, the calculation results of the two methods have the same variation trend, and the calculation errors between them are all smaller than 5.5 %.

The calculating results of d-axis super-transient reactance with different short-pitch ratios are shown in Table 7. It can be seen that the d-axis super-transient reactance increases with the short-pitch ratios increasing. The increase in the short-pitch ratios of the damping winding widens the magnetic circuit, increases the magnetic conductivity, and the reactance parameters increase accordingly [20, 21]. The conclusion is the same as that obtained by eqs. (7) and (23).

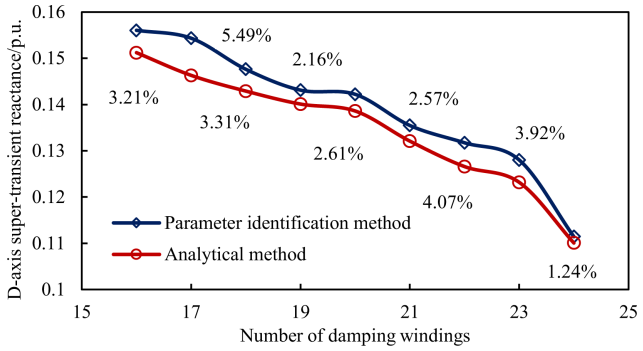

Fig. 10. (Color online) D-axis super-transient reactance with different number of damping windings.

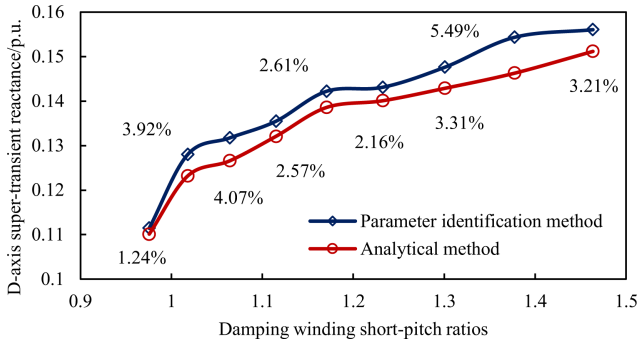

Fig. 11. (Color online) D-axis super-transient reactance with different damping winding short-pitch ratios.

Table 7. D-axis super-transient reactance with different damping winding short-pitch ratios.

Damping winding short-pitch ratios	Parameter identification method	Analytical method
0.9756	0.11146p.u.	0.1101p.u.
1.0180	0.12803p.u.	0.1232p.u.
1.0643	0.13175p.u.	0.1266p.u.
1.1150	0.13549p.u.	0.1321p.u.
1.1707	0.14222p.u.	0.1386p.u.
1.2323	0.14312p.u.	0.1401p.u.
1.3008	0.14763p.u.	0.1429p.u.
1.3773	0.15434p.u.	0.1463p.u.
1.4634	0.15605p.u.	0.1512p.u.

As can be seen in Fig. 11, the calculation results of the two methods have the same variation trend, and the errors between them are all smaller than 5.5 %.

From the above analysis results, it can be concluded that the calculation results of the two methods have the same variation law with a damping winding structure. The d-axis super-transient reactance decreases with the increasing damping winding number and increases with the increasing of short-pitch ratios. This conclusion can provide a reference for the damping winding design in DWPMEM.

6. Conclusion

This paper takes DWPMEM as the research object and proposes two d-axis super-transient reactance calculation models based on its magnetic field characteristics. The d-axis super-transient reactance with different numbers of damping windings and short-pitch ratios are calculated and analyzed by using the two models. Compared with the experimental data, it shows that the calculation results have high accuracy. The variation law of d-axis super-transient reactance with damping winding structure is investigated. The super-transient reactance calculation models proposed in this paper have important guiding significance for the design and dynamic operation evaluation of DWPMEM. It should be pointed out these models are for salient pole winding PM electrical machines with damping, and they lack universal applicability for other structures of PM electrical machines.

Based on the research foundation of this paper, further exploration can be conducted in the following two aspects: (1) Calculate other transient parameters of the d-

and q-axis by analytical method. (2) Study the relationship between the motor structural parameters and reactance parameters comprehensively, including the air gap and rotor structure *et al.* on reactance.

References

[1] Y. Tang and C. Wang, Dynamic Analysis of AC Motor, China Mach. Pre. 25 (2015).
[2] J. Gao, X. Wang, and F. Li, Analysis of Ac Motor and Its System, Tsinghua Univ. Pre. 34 (2005).
[3] A. A. Afanasiev and A. Yu. Afanasiev, Russian Elec. Eng. **90**, 565 (2019).
[4] A. A. Afanasiev, Russian Elec. Eng. **91**, 772 (2021).
[5] B. Ge, Y. Yu, Y. Liang, and F. Li, Proc. CSEE **12**, 80 (2005).
[6] W. Zhou, Elec. Mach. Ctrl. Appl. **46**, 66 (2019).
[7] J. Zhou, HUST, 2019.
[8] GB/T 1029-2021, Three-ph. Sync. Mot. Exptl. Meth. 2021.
[9] D. Liu, IEEE Trans. Appl. Supercon. **31**, 1 (2021).
[10] M. Cisneros-González and C. Hernandez, IEEE Trans. Energy Convers. **28**, 44 (2013).
[11] M. A. Arjona, IEEE Trans. Ind. Electron. **58**, 486 (2011).
[12] S. Sun, F. Jiang, and T. Li, IEEE Trans. Appl. Supercon. **30**, 6 (2020).
[13] L. Jia, K. Lin, and M. Lin, IEEE Trans. Appl. Supercon. **31**, 5 (2021).
[14] J. Zhao, X. Quan, and X. Sun, IEEE Trans. Appl. Supercon. **30**, 36 (2020).
[15] C. Gao, Z. Miao, and H. Cheng, Proc. CSEE **38**, 04 (2023).
[16] Z. Zhang, J. Jiang, and X. Zhang, Elec. Mach. Contr. **26**, 10 (2022).
[17] K. W. Klontz, T. J. E. Miller, and M. I. McGil, IEEE Trans. Ind. Appl. **47**, 4 (2011).
[18] Y. Ma, L. Zhou, and J. Wang, Trans. China Elec. Soc. **34**, 4890 (2019).
[19] Y. Ma, L. Zhou, and J. Wang, Tran. China Elec. Soc. **35**, 1208 (2020).
[20] Z. Cheng, HUST, 2018.
[21] X. Cheng, HUST, 2016.